Proceedings of the ASME 2021
Fluids Engineering Division Summer Meeting
FEDSM2021
August 10-12, 2021, Virtual, Online

FEDSM2021-65540

THE FOUR STAGE DEVELOPMENT OF STARTING TURBULENT BUOYANT PLUMES

Thanh Tran [1] and. Kiran Bhaganagar[2]
[1:] NASA CAMEE Graduate Research Assistant, Turbulence, Sensing and Intelligence Systems Laboratory, Department of Mechanical Engineering

[2:] Professor, Department of Mechanical Engineering
Turbulence, Sensing and Intelligence Systems Laboratory
Department of Mechanical Engineering, University of Texas, San Antonio (UTSA), TX,78249, USA, Email: kiran.bhaganagar@utsa.edu

ABSTRACT

Turbulent heated and buoyant plumes have important applications in the atmosphere such as wildland fire plumes, volcanic plumes, and chemical plumes. The purpose of the study is to analyze the turbulence structures, and to understand the stages of the development of the starting turbulent plumes. For this purpose, data generated from an in-house Weather Research Forecast model coupled with Large-eddy simulation (WRF-bLES) with two-way feedback between the buoyant plume and the atmosphere developed has been used. The release of both dense gases (Co2, So2) and, buoyant gases (He, NH3, heated air) from a circular source at the bottom of the domain have been investigated. The simulations of the axisymmetric plume were performed at a high Reynolds number of 10^8. Vortex Identification methods were used to extract the Coherent structures and the large-scale features of the flow. The results have demonstrated that both the dense and the buoyant heated plumes with different initial characters exhibited universal characteristics and the development of the starting plumes occurred in four characteristic stages: Stage 1 is the plume acceleration stage, followed by stage 2 which corresponds to the formation of the head of the plume which grows spatially. Stage 3 is when the plume head is fully formed and the flow transitions to quasi-steady-state behavior. The final stage is the fully developed plume.

The identification of the four-stage development of the plume in the neutral environment is the first step in studying the turbulent heated and buoyant plumes development in order to characterize realistic plumes and to quantify the extent of mixing at each of these stages. This work has important contributions to fundamental fluid dynamics of buoyant plumes with implications on forecasting the plume trajectory of smoke, wildland fire, and volcanic plumes.

NOMENCLATURE

D	sources surface diameter
λ_2	lambda 2
R_0	gas constant of the source fluid
H_0	constant surface heat flux
g'_T	reduced gravity of temperature
g'_ρ	reduced gravity of density
g'_{T_0}	initial value of reduced gravity of temperature
g'_{ρ_0}	initial value of reduced gravity of density
W_{cm}	maximum centerline *w (axial)* velocity
W_f	front velocity
z_{wcm}	z-axial location of W_{cm}
l_{wcm}	plume half-width at W_{cm}
Re_{wcm}	Reynold's number based on W_{cm}
w_b	buoyant velocity
Fr_{wcm}	Froude number
ν	viscosity of the source fluid
u_r	radial velocity of polar coordinate
u_θ	angular velocity of polar coordinate
ρ	density

1. INTRODUCTION

Wildland fire (WF) had been one of the biggest natural disasters that have a significant impact on air quality, climate, and human safety. One phenomenal fluid dynamics characteristic of the WFs is the presence of large fire whirls created by turbulent plumes rising into the atmosphere (Church, Snow & Dessens, 1980). As the plume expands into the atmosphere, due to the interaction of ambient air with the plume, the instabilities result in the formation and merging of vortex rings or whirls near the central core of the plume (Catalano, F., Moeng 2010). These large fire whirls increase the WF spreading range significantly resulting in complex fire behavior that is difficult to predict (Forthofer, Jason & Scott 2011).

Whirling behavior is observed in turbulent thermal and buoyant plume where the buoyancy force from the source creates axially aligned vortices with the surrounding air feeding into the plume and resulting in mixing within the core of the plume. In this study, turbulent thermal and buoyant plumes generated from a large-scale simulation by the Weather Research Forecast model coupled with a Large-eddy simulation (WRF-bLES) are analyzed. WRF-bLES is an in-house tool developed to simulate the two-way dynamic interactions between the atmosphere and the plume (Bhaganagar & BhimiReddy, 2020; BhimiReddy & Bhaganagar, 2018). The analysis has been conducted for five different source conditions obtained by varying the gas released at the source. The cases are classified as the release of (A) denser than ambient source fluid (So_2 and Co_2), (B) lighter source fluid (He and NH_3 and heated air). The focus of this study is to understand the stages of the development of a starting, turbulent, axisymmetric buoyant plume released from a circular source, and to quantify the plume characteristics through flow visualization techniques.

2. DATA AND METHODS

2.1 Simulation and Raw Data

WRF-bLES uses compressible Euler conservative equations in flux formulation to solve for the conservation of mass, the conservation of momentum and the conservation of energy in the model domain. The model equations are solved using a finite difference method with staggered positioning of variables. The spatial derivatives are estimated using a fifth-order accurate upwind approximation for horizontal, and third-order accurate for vertical terms. The time-split integration based on a regular third-order Runge–Kutta scheme is used to march the model equations forward in time (Bhaganagar & BhimiReddy, 2020). The physical domain of simulation is 7km (height) x 1.8km x 1.8km (horizontal direction). A circular source is placed at the bottom center of the bottom surface. The diameter of the circular source (*D*) of the released gas 400 meters. The buoyancy generated at the source is characterized using the difference in the density difference between the gas at the source and the ambiance and the temperature difference between the gas at the source and the ambiance. The coordinate system is *x, y* along the direction and *z* along the axial or vertical direction. The corresponding axial velocity is *w*, the horizontal velocity is *u* and *v*, respectively. The mesh resolution is 40 meters in the horizontal direction and 10 meters in the vertical direction. The ambient condition is still air maintained at a constant temperature of 300K.

2.2 Data Processing

A threshold criterion based on reduced gravity g'_T was used to identify the plume interface. The plume interface is obtained using the 0.01% threshold criterion of normalized g'_T. The, *u, v, w* velocity data were used to calculate λ_2 vortex criteria. λ_2 vortex criteria is a vortex visualization technique based on using minimum pressure criterion to define a vortex, but it ignores the unsteady strain rate and viscosity to define a vortex (Jeong & Hussain 1995). Using λ_2 vortex criteria, three-dimensional Iso-surface visuals were generated.

2.3 Numerical Analysis

The details of the five cases analyzed in this study are shown in Table 1. There are two inputs for the simulation: initial gas constant, R_0, and constant surface heat flux, H_0, shows in table 1. H_0 is the constant heat flux of the surface diameter *D* at the bottom boundary. The heating causes a temperature difference between the ambient fluid and the source region, which is represented by the reduced gravity g'_T (Eq. 3). The case of thermal plume serves as control data case, where the source buoyancy is generated due to the surface heat flux. The buoyancy flux is represented as the reduced gravity based on gas density, g'_{ρ_0}(Eq. 4). The negative value of g'_{ρ_0} means the gas in the plume is heavier than background air resulting in the slumping of the plume to the ground. Using the plume boundary interface, the height of the plume was measured at each instantaneous data time-step. The plume's front is defined as the distance of the leading front of the plume from the source in the axial direction at that given time, and the front speed of the plume is measured as the difference in the plume height between each time-step divided by the time step. A time-averaged front velocity, W_{fs}, is used to characterize the plume stage. Another important velocity that is used to characterize the plume is the time-averaged maximum centerline velocity, W_{cm}. Based on W_{cm}, the radial half plume-width, l_{wcm}, of the plume is measured at the corresponding axial location of W_{cm}. Reynold number of each case was calculated based on the maximum centerline velocity, W_{cm} velocity, ν viscosity, and the l_{wcm} half plume-width (1) (Bhaganagar, K., & Bhimireddy 2020). Froude number (*Fr*) is defined as the ratio of the W_{cm} to the buoyance velocity, which is estimated as $W_b = \sqrt{g'_{To} * \mathrm{D}}$.

$$Re_{wcm} = \frac{W_{cm} * l_{wcm} * D}{\nu} \quad (1)$$

$$Fr = \frac{W_{cm}}{W_b} \quad (2)$$

$$g'_{\mathrm{T_0}} = g \cdot \frac{\mathbf{\Delta T}}{T_0} \quad (3)$$

$$g'_{\rho_0} = g \cdot \frac{(\rho_{air} - \rho_{gas})}{\rho_{air}} \quad (4)$$

3. RESULTS AND DISCUSSION

Figure 1 shows the front velocity plot of the five cases which are So_2, Co_2, He, NH3, and thermal plume (Fig. 1a, 1b, 1c, 1d, and 1e respectively). The *x*-axis of each plot is the instantaneous frontal velocity of the plume, W_f, and the *y-axis* is the time in seconds from the initial release time. As shown in these plots of five cases, after initial transience, the plumes go through an acceleration stage and reach a peak velocity. The time taken to reach the peak velocity varies with each case. The Co_2 plume and the NH_3 plume reach the highest velocity the fastest, followed by He and thermal plume, respectively for the light gas cases. This is reasonable, though Co_2 is a heavier gas than NH_3, the initial heat flux of Co_2 is twice the initial heat flux of NH_3 which balanced out the negative buoyant flux of the Co_2. When comparing the lighter gases with each other, the initial gas flux NH_3 is higher than that of He and resulting in a higher buoyancy flux. On the other hand, for the dense gas cases, the Co_2 plume reaches the peak front velocity much faster than the So_2 case. Similarly, due to higher initial heat flux at the source, So_2 accelerates much faster compared to Co_2. After the initial stage, the plume transitions into the deceleration stage, and then followed by the quasi-steady stage, and finally the steady stage, which is the fourth stage. The analysis of each of these stages is explained next.

	Dense gas		Lighter gas		
	Case 1	Case 2	Case 3	Case 4	Case 5
Gas released	So_2	Co_2	He	NH_3	Thermal Plume
R_0 (J/kg·k)	129.78	188.92	2077.1	488.21	287.00
H_0 (kms^{-1})	2.5	5.0	2.0	2.5	0.5
$g'_{T0}(ms^{-2})$	0.1962	0.5029	0.2006	0.1850	0.0820
$g'_{\rho 0}(ms^{-2})$	-11.24	-6.04	8.49	2.92	0.00
$W_{fs}(s^{-1})$	0.0025	0.0054	0.0037	0.0057	0.033
$W_{cm}(ms^{-1})$	1.760	12.710	4.700	14.320	5.760
z_{wcm}	2.275	1.675	2.000	3.700	1.625
l_{wcm}	0.900	0.600	0.900	1.100	0.6292
Re_{wcm}	4.04e7	1.94e8	1.08e8	4.01e8	9.23e7
$w_b(s^{-1})$	8.8589	14.183	8.9577	8.6023	5.7271
Fr	0.1988	0.8962	0.5248	1.6649	1.0049

TABLE 1. Initial conditions and dimensionless number for simulated plume cases.

a) Case1:
So_2 *front velocity. (R_0: 129.78 J/kg·k, H_0: 2.5* kms^{-1}*)*

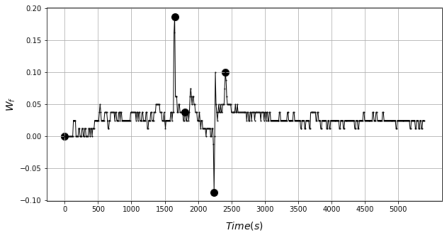

b) Case2:
Co_2 *front velocity. (R_0: 188.92 J/kg·k, H_0: 5 kms^{-1})*

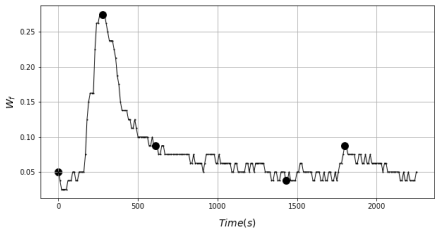

c) Case 3:
He front velocity. (R_0: 2077.1 J/kg·k, H_0: 2 kms^{-1})

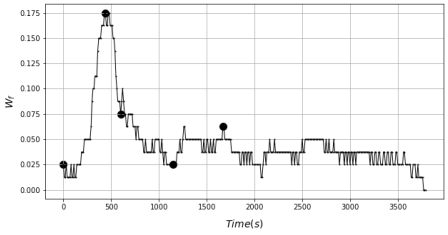

d) Case 4:
NH3 front velocity. (R_0: 488.21 *J/kg·k, H_0: 2.5 kms^{-1})*

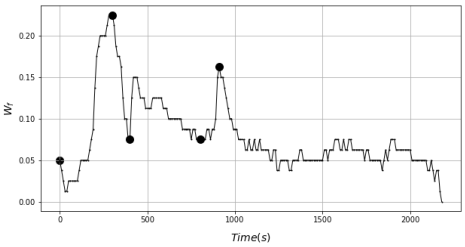

e) Case 5:
Thermal Plume front velocity. (R_0: 287.00 J/kg·k, H_0:0.5 kms^{-1})

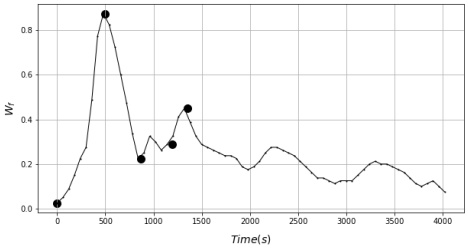

FIGURE 1: Front Velocity of Five Cases (1-5).

	Dense gas		Light gas		
	Case 1	Case 2	Case 3	Case 4	Case 5
Data Gas	So_2	Co_2	He	NH3	Thermal Plume
Stage 1	0-1650	0-280	0-440	0-300	0-500
Stage 2	1650-1800	280-610	440-600	300-400	500-865
Stage 3	1800-2240	610-1430	600-1150	400-800	865-1195
Stage 4	2240-2410	1430-1800	1150-1670	800-910	1195-1275

TABLE 2. Timestamp in second for each stage of the turbulent thermal plume.

3.1 Stage One

Stage one is defined as the initial stage of the plume during which the plume accelerates from the starting point to the point at which the plume reaches its maximum front velocity. This is the acceleration stage. During this stage, the turbulent plume rises axially without significant radial expansion. This trend is observed in all the cases. It should be noted that the trend of the front velocity of case 1 and case 2 is different compared to the lighter cases the heavier gases tend to slump together the ground due to their weight.

In Figure 2, the λ_2 Isosurface of λ_2 during stage 1 for case 3 (Co_2) is shown. A blob-shaped plume structure is formed, and it is relatively undiluted at this stage. Due to the limitation of the space, only one case is represented here. However, a similar trend is observed for all five cases.

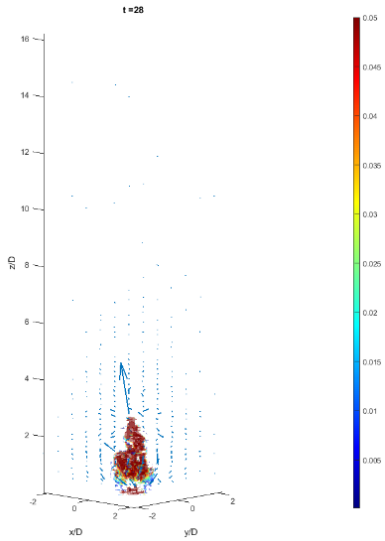

FIGURE 2: During Stage 1 the λ_2 Isosurfaces overlayed on velocity vectors for Case 2 (Co_2) plotted at time = 280s.

3.2 Stage Two

The second stage is defined as the duration during which the plume head forms as seen in Fig.3. The formation of the head corresponds to the deceleration of the plume front as seen in Fig.1. During this stage, a well-defined circular vortex structure is evident (e.g., at z = 2.5*D*, 6.7*D*). There is significant mixing that is initiated. Close to the source, the plume relatively is well unmixed, however, in the bulged region corresponding to the head, the mixing is very significant resulting in the dilution of the plume. To extract the circular flow characteristics, the velocity vectors are represented in polar coordinates. Fig.4 shows the velocity vectors of u_r and u_θ at *z/D*=7, showing the circulation around the centerline.

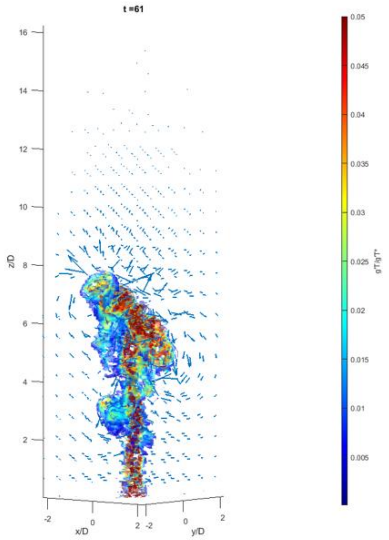

FIGURE 3: During Stage 2 the λ_2 Isosurfaces overlayed on velocity vectors for Case 2 (Co_2) plotted at time = 610s.

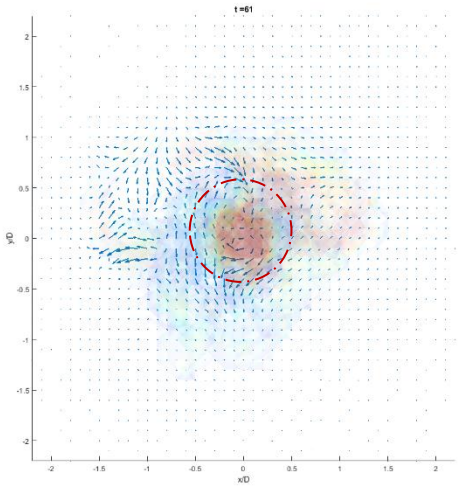

FIGURE 4: During Stage 2, Top View of Polar Coordinate Quiver Plot, Case 2 (z/D = 7) at time = 610s.

3.3 Stage Three

The third stage is defined as the stage when the plume head is fully formed and the flow transitions to a quasi-steady-state behavior. The front reaches a quasi-steady stage with the average front velocity varying as 0.0025 and 0.0054 for case 1

and case 2, respectively, and with values of 0.0036, 0.0057, and 0.0181 for cases 3, 4, and 5, respectively. The final steady-state front velocity correlates with the initial heat flux and the gas constant. The lighter the fluid, the higher is the surface heat flux and the higher is the steady-state front velocity. A similar trend is clear for the dense gases. The surface of the λ_2 overlaid on the velocity vectors is shown in Fig.5. During this stage, the mixing or entrainment is significantly enhanced resulting in the dilution of the plume. A fully developed plume is formed. The ambient fluid enters the plume near the leading edge of the front in the head region of the plume.

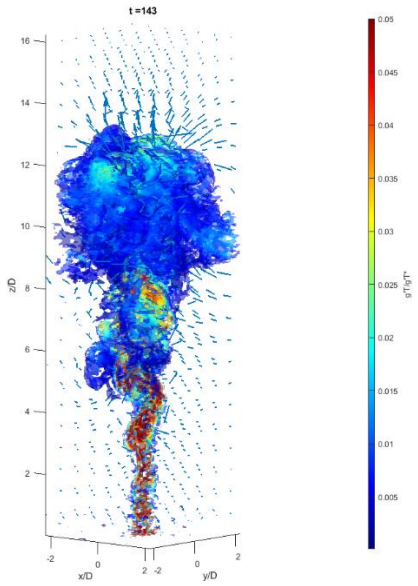

FIGURE 5: During Stage 3 the λ_2 Isosurfaces overlayed on velocity vectors for Case 2 (Co_2) plotted at time = 1430s.

3.4 Stage Four

The final stage is the fully developed plume. At this stage, the plume is now of two distinct regions: close to the source is the relatively undiluted region the width of which is the size of the diameter of the source, the undiluted cylindrical region is capped by a head region that is unstable resulting in drastic mixing, as seen in separated into two different segments, Fig.6. The upper region is the plume head with jet-like characters. Meanwhile, the bottom region is taking a shape of an elongated cylindrical tube and slowly transforming as a sigmoid function into the head of the plume.

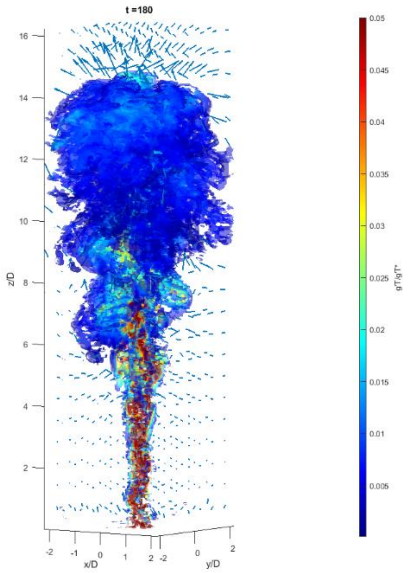

FIGURE 6: During Stage 4 the λ_2 Isosurfaces overlayed on velocity vectors for Case 2 (Co_2) plotted at time = 1800s.

4. CONCLUSION

In this study, flow visualization analysis has been conducted to understand the development stages of starting buoyant plumes for both dense and lighter plumes released into the atmosphere. The results have demonstrated that thermal plumes, dense and buoyant plumes all exhibit universal characteristics, and the development of the starting plumes occurs in four characteristic stages. The identification of the four-stage development of the turbulent plume in a neutral environment has important significance to characterize realistic plumes and to quantify the extent of mixing at each of these stages. The work has important contributions to our fundamental understanding of the fluid dynamics of buoyancy driven plumes, and with implications in the forecasting of the plume trajectory of smoke, wildland fire, or volcanic plumes.

REFERENCES

[1] Church, C. R., J. T. Snow, and J. Dessens, 1980: Intense atmospheric vortices associated with a 1000 MW fire. *Bull. Amer. Meteor. Soc.*, **61**, 682–694.

[2] Bhaganagar, K., & Bhimireddy, S. (2020). Numerical investigation of starting turbulent buoyant plumes released in a neutral atmosphere. Journal of Fluid Mechanics, 900, A32. doi:10.1017/jfm.2020.474

[3] Catalano, F., Moeng, CH. Large-Eddy Simulation of the Daytime Boundary Layer in an Idealized Valley Using the Weather Research and Forecasting Numerical Model. Boundary-Layer Meteorol 137, 49–75 (2010). https://doi.org/10.1007/s10546-010-9518-8

[4] Forthofer, Jason & Goodrick, Scott. (2011). Review of Vortices in Wildland Fire. Hindawi Publishing Corporation Journal of Combustion. 14. 10.1155/2011/984363

[5] Jinhee Jeong, Fazle Hussain, 1995 On the identification of a vortex J. Fluid Mech., pp.69-94

[6] Bhimireddy, Sudheer & Bhaganagar, Kiran, Short-term passive tracer plume dispersion in convective boundary layer using a high-resolution WRF-ARW model, *Atmospheric Pollution Research, 9:901-911, 2018*